



## **ICATE 2002**

**UNIVERSITY OF CRAIOVA  
FACULTY FOR ELECTRICAL ENGINEERING  
FACULTY FOR ELECTROMECHANICAL ENGINEERING**

# **PROCEEDINGS**

**ON THE**

**INTERNATIONAL CONFERENCE ON APPLIED  
AND THEORETICAL ELECTRICITY**

**CRAIOVA / BAILE HERCULANE, OCTOBER 17 – 19, 2002**

**ROMANIA**

---

**UNIVERSITARIA PUBLISHER**

2.6	Influence of Reaction Field Upon Dynamic Regime of Separately Excited Direct Current Motor Ion VLAD; Sorin ENACHE	109
2.7	Aspects Regarding Determination of The Characteristics of Induction Motors by Voltage Converter of High Performance Decebal ALEXANDRU; Sonia DEGERATU; Marian GAVRILA; Paul MARINAS	115
2.8	Computerized Micro-Stand for the Study of Asynchronous Motor Operation Sorin ENACHE; Ion VLAD ; Monica-Adela ENACHE	121
2.9	Study of Asynchronous Motor by Graphic Language Alina VIOREL, Mihai Paun	125
2.10	The Orthogonal Model Of The Synchronous Machine And The Modelling Of The Asynchronous Machine Gheorghe SAMOILBESCU; Silviu GHEORGHIU	129

### Section 3 ELECTRICAL DRIVES

3.1	Reglage Automate de la Position par Mode de Glissement avec Moteur a Courant Continu et Frein Mihaela POPESCU ; Alexandru BITOLEANU; Mircea DOBRICEANU; Octavian POPESCU	137
3.2	A Fuzzy Direct Torque Control of A PWM-Inverter-Fed Induction Machine Drive Daniel PIRJAN ; Francis LABRIQUE; Damian GRENIE	143
3.3	Comparasion of the Rotor Flux and Magnetising Flux Oriented Vector Controls of the VSI Induction Motor Drives Sergiu IVANOV	149
3.4	Comparative Analysis of Control Structures with Internal Model and with Perturbation Observer Vasile BAHRIN; Carmen COJOCARU-FILIPCIUC	155
3.5	Neuro-Fuzzy Modelling for A Dc Motor Cătălin CONSTANTINESCU; Dan MIHAI	159
3.6	A Neuro-Fuzzy Model for A DC Motor in Standard and Fuzzy Position Control Loops Dan MIHAI; Cătălin CONSTANTINESCU	165
3.7	A Simplified Space Vector Modulation Technique for A VSI-FED Induction Motor Drive Marian BADICA	171

### Section 4 ELECTRICAL APPARATUS. HIGH VOLTAGE EQUIPMENTS

4.1	A Physical Semnification of the Instantaneous Characteristic Impedance Gleb DRAGAN	179
4.2	Determination of Lightning Rod Protection Areas Using Probabilistic Model Sensitivity Of Solutions Gleb DRAGAN; Petru POSTOLACHE; Vasile RAMNICEANU	183
4.3	Influence of an Earthed Circular Conductor on the Bus - Bars Dragutin M. VELIČKOVIĆ, Nenad N. CVETKOVIĆ	187
4.4	Inductance of A Plunger-Type Electromagnet Grigore CIVIDJIAN; Alin DOLAN; Victor CLIMOV; Ali Ihsan CANAKOGLU	193
4.5	Initial Voltage Distribution on Two Capacity Coupled Transformer Windings Grigore CIVIDJIAN; Gheorghe CALIN; Dorin POPA	199
4.6	Methodes Des Volumes Finis Appliquees aux Problemes de Convection- Diffusion 1D Stationnaires Ioan POPA	203
4.7	Controllable Current Stabilized Source Of 0-10ka to Stands for HV Switchgear Heating Test Dorel NEDELICUT; Gheorghe FLORIGANTA ; Victor PROCA; Adrian VINTILA	209
4.8	Metrological Verification of Shunts and Rogowski Coils in the Range 2-200 KA Horia IONESCU, Alexandru MANTA; Mircea ISTRATE	213

## INDUCTANCE OF A PLUNGER-TYPE ELECTROMAGNET

Grigore A. CIVIDJIAN, Alin DOLAN, Victor CLIMOV, Ali Ihsan CANAKOGLU\*

*University of Craiova, Romania,\* Dumlupinar University, Kutahya, Turkey  
Lapus 5, RO-1100 Craiova, Tel: +40251/435724, E-mail : gcividjian@elth.ucv.ro*

### Abstract

In the paper, an experimental and FEM verification of early obtained, internal inductance formula for plunger type magnet is performed. A new, faster, method for the calculation using Mathcad is substantiate and recommended.

### 1. - INTRODUCTION

In [1] a formula for internal inductance of plunger-type magnet is deduced, using the method of power approximation of boundary conditions in 2D connected regions. The proposed formula, which takes into consideration the core saturation, the parasite air gaps and the variation in large limits of the working gap, is difficult to apply because of the function

$$F(\alpha, z) = \int_0^1 \frac{\cos[z(1-t)]}{t^\alpha} dt; \quad \alpha \in (0,1) \quad (1)$$

containing an improper integral.

In the paper, a method for the evaluation of this function, using Mathcad, is proposed and two verifications of the formula are performed: using a finite element method and experimental determinations of the total inductance for large range of the gap variation. The experimental values are compared with the sum of internal inductance, calculated with formula given in [1] and external inductance calculated with finite element method (Quickfield and femm).

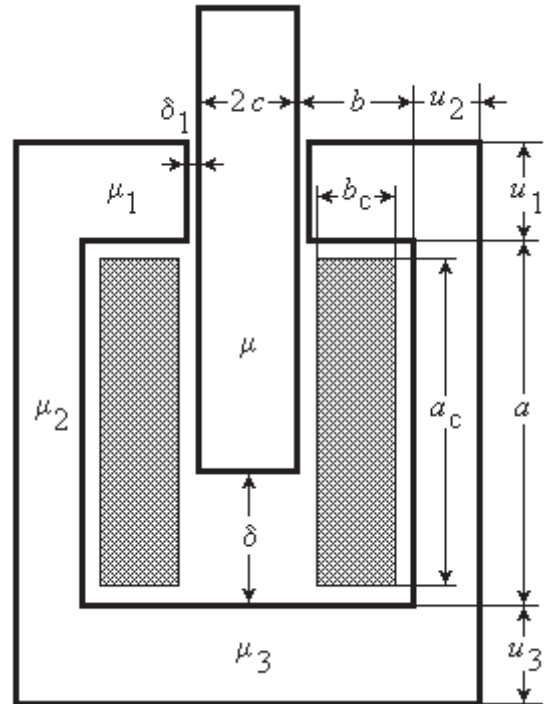


Fig. 1 Plunger - Type Magnet

### 2.-CALCULATION OF $F(\alpha, z)$

The values of  $\alpha$  was taken using the recommendations given in [1]. The recommendations from [2] can be also used.

The function (1) contain an improper integral, difficult to calculate, but it can be expressed in terms of Bohmer integrals (or generalized Fresnel integrals) [3]:

$$\begin{aligned} C(x, \alpha) &= \int_x^\infty \frac{\cos t}{t^{1-\alpha}} dt; & S(x, \alpha) &= \int_x^\infty \frac{\sin t}{t^{1-\alpha}} dt \\ C(x, \alpha) &= \frac{1}{2} \left[ e^{-\frac{i\pi\alpha}{2}} \Gamma(\alpha, ix) + e^{\frac{i\pi\alpha}{2}} \Gamma(\alpha, -ix) \right] \\ S(x, \alpha) &= \frac{1}{2i} \left[ e^{\frac{i\pi\alpha}{2}} \Gamma(\alpha, -ix) - e^{-\frac{i\pi\alpha}{2}} \Gamma(\alpha, ix) \right] \end{aligned} \quad (2)$$

For  $x \rightarrow 0$  we have evidently

$$\begin{aligned} C(0, \alpha) &= \Gamma(\alpha) \cos\left(\frac{\alpha \pi}{2}\right); \\ S(0, \alpha) &= \Gamma(\alpha) \sin\left(\frac{\alpha \pi}{2}\right) \end{aligned} \quad (3)$$

We will consider also the complementary integrals

$$C_0(x, \alpha) = \int_0^x \frac{\cos t}{t^{1-\alpha}} dt; \quad S_0(x, \alpha) = \int_0^x \frac{\sin t}{t^{1-\alpha}} dt \quad (4)$$

They satisfy the equations:

$$\begin{aligned} C_0(x, \alpha) + C(x, \alpha) &= C(0, \alpha) = \Gamma(\alpha) \cos\left(\frac{\alpha \pi}{2}\right) \\ S_0(x, \alpha) + S(x, \alpha) &= S(0, \alpha) = \Gamma(\alpha) \sin\left(\frac{\alpha \pi}{2}\right) \end{aligned} \quad (5)$$

For large  $x$ , the following equations can be useful [3]:

$$\begin{aligned} C(x, \alpha) &= -x^\alpha [P(x, \alpha) \sin x + Q(x, \alpha) \cos x] \\ S(x, \alpha) &= x^\alpha [P(x, \alpha) \cos x - Q(x, \alpha) \sin x] \end{aligned} \quad (6)$$

where

$$\begin{aligned} P(x, \alpha) &= \sum_{m=0}^{M-1} \frac{(-1)^m (1-\alpha)_{2m}}{x^{2m+1}} + O(|x|^{-2M-1}) \\ Q(x, \alpha) &= \sum_{m=1}^M \frac{(-1)^m (1-\alpha)_{2m-1}}{x^{2m}} + O(|x|^{-2M-2}) \end{aligned} \quad (7)$$

Here is used the Pochhammer symbol

$$(\alpha)_n = \alpha(\alpha+1)(\alpha+2)\dots(\alpha+n-1) = \frac{\Gamma(\alpha+n)}{\Gamma(\alpha)} \quad (8)$$

Using the substitution  $z t = x \Rightarrow z dt = dx$  to change the integration variable  $t$  with  $x$  in (1), the function  $F$  can be expressed in terms of the complementary integrals (4)

$$\begin{aligned} F(\alpha, z) &= \frac{1}{z^{1-\alpha}} \int_0^z \frac{\cos(z-x)}{x^\alpha} dx = \\ &= \frac{1}{z^{1-\alpha}} [\cos z C_0(z, 1-\alpha) + \sin z S_0(z, 1-\alpha)] \end{aligned} \quad (9)$$

The complementary integrals have the following series representation [3]:

$$\begin{aligned} C_0(x, \alpha) &= \sum_{m=0}^{\infty} \frac{(-1)^m x^{2m+\alpha}}{(2m)!(2m+\alpha)} \\ S_0(x, \alpha) &= \sum_{m=0}^{\infty} \frac{(-1)^m x^{2m+1+\alpha}}{(2m+1)!(2m+1+\alpha)} \end{aligned} \quad (10)$$

The above series are alternating and the truncation error is less than the first neglected term. For  $x \leq 1$ , the error, for  $(m+1)$  taken terms, is less than

$$T(m) = \frac{1}{2m(2m)!} \quad (11)$$

For error less than  $10^{-12}$  there are enough 7 terms. To avoid the calculation of improper integrals we propose to calculate the complementary integrals (4), using Mathcad, as follows:

$$\begin{aligned} C_0(x, \alpha) &= \begin{cases} C_{01}(x, \alpha) & x \leq 1 \\ C_{01}(1, \alpha) + \int_1^x \frac{\cos t}{t^{1-\alpha}} dt & x > 1 \end{cases} \\ S_0(x, \alpha) &= \begin{cases} S_{01}(x, \alpha) & x \leq 1 \\ S_{01}(1, \alpha) + \int_1^x \frac{\sin t}{t^{1-\alpha}} dt & x > 1 \end{cases} \end{aligned} \quad (12)$$

where

$$\begin{aligned} C_{01}(x, \alpha) &= \sum_{m=0}^6 \frac{(-1)^m x^{2m+\alpha}}{(2m)!(2m+\alpha)} \\ S_{01}(x, \alpha) &= \sum_{m=0}^6 \frac{(-1)^m x^{2m+1+\alpha}}{(2m+1)!(2m+1+\alpha)} \end{aligned} \quad (13)$$

The integrals in equations (12) are not improper and can be easily calculated with good precision by Mathcad. The values of the function  $F$  calculated with (9), (12) and (13) are given in fig. 2.

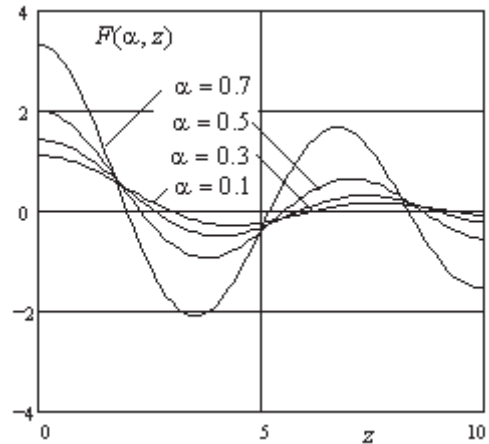


Fig. 2. The function  $F(\alpha, z)$

The function  $F$  can be easily calculated also using the equations (6). Replacing (6) in (5) and (9) we obtain:

$$F(\alpha, z) = \frac{\Gamma(\alpha)}{z^{1-\alpha}} \cos\left(\frac{\alpha \pi}{2} - z\right) + Q(z, 1-\alpha) \quad (14)$$

The last term, in accordance with (7) can be written as

$$Q(z, 1-\alpha) \cong \sum_{m=1}^M \frac{(-1)^m \Gamma(\alpha + 2m - 1)}{z^{2m} \Gamma(\alpha)} \quad (15)$$

For  $z > 10$  it can be calculated with an absolute error less than  $10^{-12}$ , if  $M = 5$ .

The values of  $-Q(z, 1-\alpha)$  are given in fig. 3. We can see that for large  $z$  this term can be neglected. In the program given in appendix of [1] this term is neglected, for  $z$  larger than 90. This corresponds to an absolute error smaller than  $10^{-4}$ .

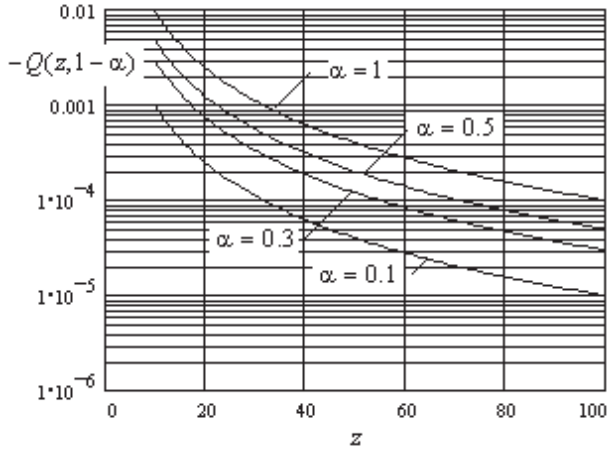


Fig. 3. The function (15)

### 3. – INTERNAL INDUCTANCE

The inductance corresponding to the magnetic flux in the two windows of the magnet (fig. 1) according to [1], can be written in the form

$$L_{\text{int}} = 2\mu_0 w^2 \left[ G + \frac{c}{\delta_e} + \frac{a_1 a + b_1 b}{2\delta_e} - \frac{a_2 a^2 + b_2 b^2}{6ab} \right] \quad (16)$$

In this formula the coil cross-section is considered to have the window dimensions:  $a_c \approx a$ ,  $b_c \approx b$ .

The equivalent air gap, using the notation from fig. 1

$$\delta_e = \delta + \frac{a-b}{\mu} + \frac{c}{u_1} \left( \delta_1 + \frac{b-\delta_1}{\mu_1} \right) + \frac{c}{u_2} \frac{a}{\mu_2} + \frac{c}{u_3} \frac{b}{\mu_3} \quad (17)$$

The magnetic field in various portions of the magnet can be approximated neglecting the leakage flux:

$$H_\delta = \mu H = \frac{u_1}{c} H_{\delta_1} = \frac{\mu_i u_i}{c} H_i = \frac{wI}{\delta_e}; \quad i = 1...3 \quad (18)$$

The coefficients  $a_i$  and  $b_i$  have the expressions [1]:

$$a_1 = \frac{c}{\mu_3 u_3}; \quad a_2 = \frac{1}{\delta_e} \left[ \frac{c}{u_1} \left( \delta_1 + \frac{b-\delta_1}{\mu_1} \right) + \frac{b}{\mu_3} \frac{c}{u_3} \right] \quad (19)$$

$$b_1 = \frac{1}{a} \left( \delta + \frac{a-\delta}{\mu} \right); \quad b_2 = \frac{1}{\delta_e} \left[ \delta + \frac{a-\delta}{\mu} + \frac{a}{\mu_2} \frac{c}{u_2} \right]$$

The interpolation coefficients can be selected following the recommendations [1]:

$$k_1 = 1 - \frac{1}{6\alpha}; \quad k_2 = \frac{1-\alpha}{6\alpha}$$

$$\alpha = 0.44 + 2.2(\delta/a) - 2.68(\delta/a)^2 \quad \text{for } b/a = 0.10 \quad (20)$$

$$\alpha = 0.42 + 1.80(\delta/a) - 2.20(\delta/a)^2 \quad \text{for } b/a = 0.15$$

$$\alpha = 0.41 + 1.29(\delta/a) - 1.60(\delta/a)^2 \quad \text{for } b/a = 0.25$$

$$\alpha = 0.44 + 0.70(\delta/a) - 1.15(\delta/a)^2 \quad \text{for } b/a \geq 0.50.$$

or, for larger gaps, the recommendations [2]:

$$k_1 = 1 - \frac{1-u_0}{\alpha}; \quad k_2 = (1-u_0) \frac{1-\alpha}{\alpha}$$

$$u_0 = 0.831957 + 1.54394 \cdot 10^{-2} \frac{\delta}{b} - 0.175235 \left( \frac{\delta}{b} \right)^2 + 7.66579 \cdot 10^{-2} \left( \frac{\delta}{b} \right)^3 - 1.60908 \cdot 10^{-2} \left( \frac{\delta}{b} \right)^4 + 1.83817 \cdot 10^{-3} \left( \frac{\delta}{b} \right)^5 - 1.09529 \cdot 10^{-4} \left( \frac{\delta}{b} \right)^6 + 2.66537 \cdot 10^{-6} \left( \frac{\delta}{b} \right)^7 \quad (21)$$

$$\alpha = 0.3 + 0.021 \cdot \frac{\delta}{b}$$

The proper values result from the equations

$$\lambda_1 a = \lambda_2 b = v \delta = k \pi \quad (22)$$

The Fourier coefficients are

$$c_k = \frac{-2}{k\pi \text{th}(\lambda_1 b)} \left[ \left( k_1 - \frac{1}{\mu} \right) \frac{\sin(\lambda_1 \delta)}{\lambda_1 \delta_e} + k_2 \frac{\delta}{\delta_e} F(\alpha, \lambda_1 \delta) \right]$$

$$d_k = \frac{-2}{k\pi \text{th}(\lambda_2 a)} \frac{c}{u_1} \left[ \left( k_1 - \frac{1}{\mu_1} \right) \frac{\sin(\lambda_2 \delta_1)}{\lambda_2 \delta_e} + k_2 \frac{\delta_1}{\delta_e} F(\alpha, \lambda_2 \delta_1) \right] \quad (23)$$

The constant  $G$  from the equation (16) is given in fig. 3 from [1] and can be calculated, taking 10 terms in the equation:

$$G = \frac{a_2 \delta^2}{6ab} - \frac{a_1 \delta}{2\delta_e} - \sum_{k=1}^{\infty} \left[ c_k \frac{\sin(\lambda_1 \delta)}{\lambda_1 \delta} + d_k \frac{\text{sh}(\lambda_2 \delta)}{\lambda_2 \delta \text{ch}(\lambda_2 a)} \right] \quad (24)$$

#### 4. FEM AND EXPERIMENTAL VERIFICATION

For FEM and experimental verification the electromagnet shown in fig. 1 and 4, with the dimensions (in mm) given in the next table, was used

$a$	$b$	$c$	$u_1$	$u_2$	$u_3$
70	17.75	7.25	15	9	15

$g$	$\delta_1$	$w$	$a_c$	$b_c$	$R$
15.3	0.15	2350	65	13.8	100

where  $g$  is the core thickness,  $a_c$ ,  $b_c$  are the coil dimensions,  $w$  the number of turns and  $R$  the domain radius for external inductance calculation. The relative permeability was considered 1000 for all the portions of the core.

In the next table, are given the 2D magnetic field energy (per 1 m length)  $W_{\text{ext}}$  in two lateral sides of the coil up to a distance  $R = 100$  mm and the magnetic energy  $W_{\text{int}}$  in the two magnet windows, both calculated by Quickfield program for a apparent current density of 1 A/mm<sup>2</sup>, i.e. a coil current

$$I_1 = 10^6 \frac{a_c b_c}{w} = 0.382 \text{ [A]} \quad (25)$$

In next two columns the corresponding external and internal inductances in H/m are given, calculated with the formulas

$$L'_{\text{ext}} = 2 \frac{2W_{\text{ext}}}{I_1^2}; \quad L'_{\text{int}} = 2 \frac{2W_{\text{int}}}{I_1^2} \quad (26)$$

and in the last column the theoretical values calculated with the formula (16).

$\delta$ [mm]	FEM (QFLD, FEMM)				(16)
	$W_{\text{ext}}$ [J/m]	$W_{\text{int}}$ [J/m]	$L'_{\text{ext}}$ [H/m]	$L'_{\text{int}}$ [H/m]	$L_{\text{int}}$ [H/m]
2.5	0.183	2.355	5.018	64.666	66.211
5	0.173	1.564	4.761	42.941	43.951
10	0.153	1.019	4.209	27.987	28.856
20	0.126	0.654	3.459	17.955	17.228
40	0.066	0.251	1.819	6.882	7.194

We can observe in fig. 7 a good agreement with the FEM data (differences less than 4.5%).

Using the external inductances determined with FEM and the determined by FEM and calculated with equation (16) internal inductance, the total coil inductance was calculated, considering for internal inductance the core thickness  $g$  and for external inductance the rest of mean turn half length:

$$L'_{\text{tot}} = gL'_{\text{int}} + \left( \frac{l_m}{2} - g \right) L'_{\text{ext}} \quad (27)$$

$$L_{\text{tot}} = gL_{\text{int}} + \left( \frac{l_m}{2} - g \right) L_{\text{ext}}$$

$$l_m = 2(c_c + g_c) + \pi b_c$$

In the last table, these values are compared with experimental data obtained for feeding voltage  $U = 50$  V, 50 Hz and the currents  $I$  given in the table, considering the coil resistance  $R_c = 23.3 \Omega$ :

$$L''_{\text{tot}} = \frac{1}{100 \pi} \sqrt{\left( \frac{U}{I} \right)^2 - R_c^2} \quad (28)$$

The larger difference between the experimental data and calculated inductances for small air gap can be explained by the altered shape of the plunger which is not flat faced, like in fig. 1 and has also a T shape instead of I. The smaller plunger area gives a smaller inductance. This explanation is supported by the good agreement of the formula (16) results with the FEM data.

$\delta$ [mm]	$I$ [A]	$L''_{\text{tot}}$ [H]	$L'_{\text{tot}}$ [H]	$L_{\text{tot}}$ [H]	$L_{\text{tot}} / L''_{\text{tot}}$
2.5	0.158	1.005	1.214	1.238	1.232
5	0.193	0.821	0.870	0.885	1.078
10	0.251	0.630	0.617	0.630	1
20	0.377	0.416	0.403	0.418	1.007
40	0.814	0.181	0.187	0.191	1.057

For gaps larger than 5 mm the differences are smaller than 8 %, which can be considered acceptable.

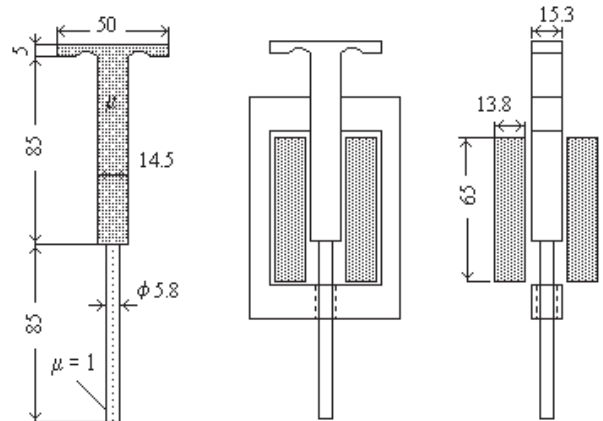


Fig. 4 The experimental model

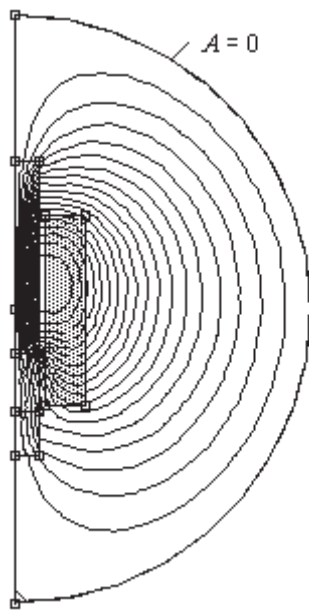


Fig. 5. External magnetic field for the gap 20 mm

$$W_{\text{ext}} = 0.126 \text{ J/m}, w I = 898 \text{ A}$$

1352 nodes, 2547 elements

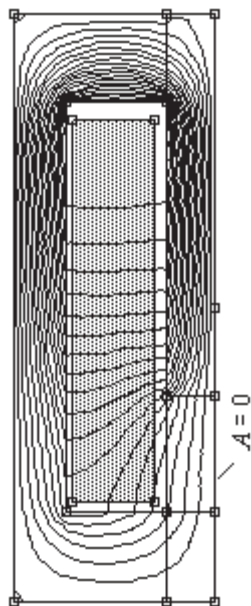


Fig. 6 Internal magnetic field for the gap 20 mm

$$w I = 898 \text{ A}, W_{\text{int}} = 0.654 \text{ J/m}$$

1444 nodes, 2730 elements

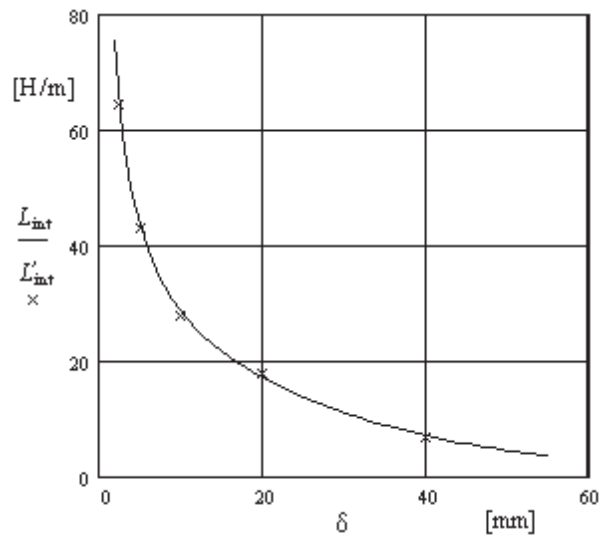


Fig. 7. Internal inductance calculated with (16) (line) and determined by FEM (x's)

## 5. – DELPHI PROGRAM

A user-friendly Delphi program (called IPTM.exe) was built by the last co-author, which determine very fast the constant  $G$  and internal inductance  $L_{\text{int}}$  using the formulas (16) and (24) and given in [1] algorithm for  $F$  function calculation.

The program calculates also the vector magnetic potential for given points in the two domains: I – coil cross-section and II – the air gap. The results can be stored in text files and the graphics in bmp. Files. Four (color) menu pages offered by this program are shown in the next several figures.

**Inductance of a Plunger-Type Magn** \_ | □ | ×

Variables | Graphic (G) | Graphic (L) | Vector Potentials |

a:	0.070
b:	0.01775
c:	0.00725
$\mu$ :	1000
$\mu_1$ :	1000
$u_1$ :	0.015
$u_2$ :	0.009
$u_3$ :	0.015
$\delta$ :	0.020
$\delta_1$ :	0.00015
I:	0.377
$\omega$ :	2350

Increment of  $\delta/a = 40$

To Compute with new values Click here.....>> Graphic >>

Read from File | Save to File | Exit

Fig. 8. Delphi program main menu

In fig. 8 the dimensions of the experimental model are introduced.

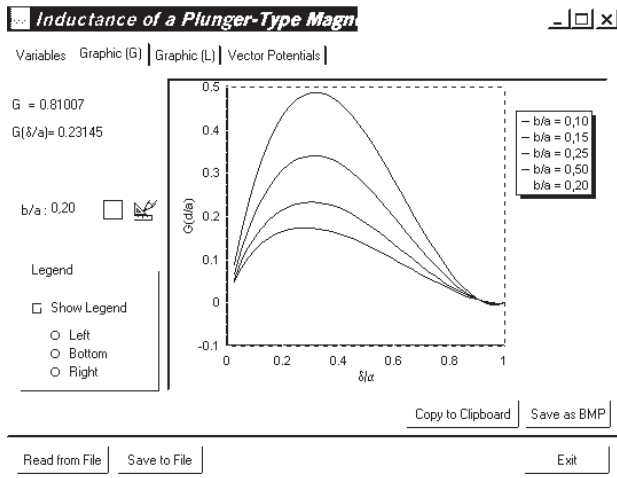


Fig. 9. The parameter  $G \frac{\delta}{a}$  as a function of  $\frac{\delta}{a}$  for four ratio of window dimensions

In the figure above the constant  $G$  is calculated for four shapes of the rectangular window.

The time need to calculate the graphics for  $G$  is around 4 seconds, for a computer with 800 MHz processor. The next menus are almost instantaneous.

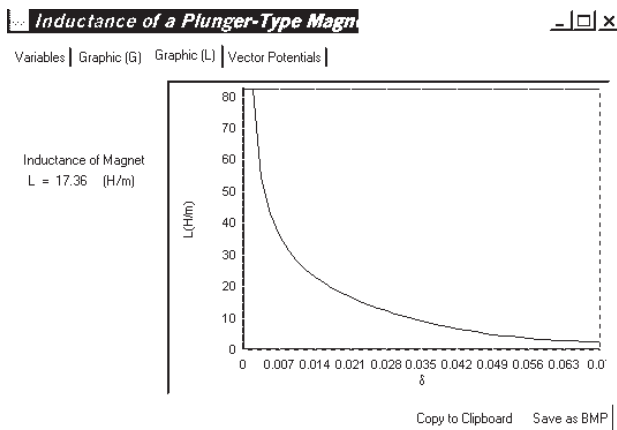


Fig. 10. The internal inductance  $L_{int}$  as a function of the gap

The next menu calculates the vector magnetic potential in the two domains (core window and air gap), i. e. the magnetic flux per 1 m depth, between the zero flux line ( $A = 0$  in fig. 6) and the selected point, in [Wb/m].

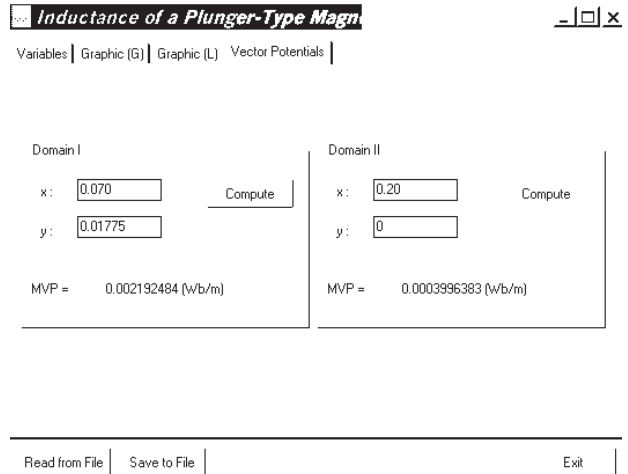


Fig. 11. The magnetic vector potential values

## 6 - CONCLUSIONS

1. The formula (16), considering the coil cross-section equal to window dimensions, gives the values of the internal partial inductance of plunger-type electromagnet which are in good agreement with the values obtained using FEM method (differences less than 4.5 %).
2. For total magnet inductance evaluation, two values of linear inductances can be considered: internal inductance  $L_{int}$ , which must be multiplied by the core thickness  $g$  and the external inductance  $L_{ext}$ , which must be multiplied by the rest of the mean turn of the coil length (27).

## ACKNOWLEDGEMENT

The authors gratefully acknowledge professor Ivan Yatchev from Technical University of Sofia for the help in program Femm implementation and assimilation.

## REFERENCES

1. G. A. Cividjian et al., *Inductance of a plunger-type magnet*, IEEE Trans. on Magnetics, vol. 34, no. 5, Sept. 1998, pp. 3695-3688.
2. G. A. Cividjian et al., *Power Approximation of Boundary Conditions*, Seconde Conf. Europeenne sur les Methodes Numeriques en Electromagnetisme, Lyon, 19-21 Mars 1997, NUMELEC 97, 252-253.
3. H. Bateman, A. Erdelyi, *Higher Transcendental Function*, vol . 2, Mc. Graw-Hill, N. Y., 1953